Kodaikanal Obs. Bull. (1993) 12, 93-100

Compton Broadening Due To Electron Scattering

A.Peraiah and M.Srinivasa Rao

Received 22nd Sep 1993 , accepted 5th Oct 1993

Abstract

We have investigated the effects of Compton broadening due to electron scattering in the hot stellar atmospheres, quasars, AGN's etc. We considered a purely electron scattering media. The Compton effect scattering function produces the redshift and asymmetry in the line. These two effects increase as the optical depth increases. For an optical depth of 100, the emergent specific intensities become completely asymmetric in a given direction.

Key words: Compton broadening-Electron Scattering

1. Introduction

Electron scattering appears to have considerable influence through Compton broadening in the formation of spectral lines in objects such as the outer layers of hot stars, AGN's, Seyfert galaxies etc. Electron scattering contributes not only to the opacity of high temperature stellar atmospheres but also produces broadening and asymmetry in the spectral lines of such stars. The redistribution of photons in the line are due to Doppler motion of the electrons and the Compton effect in the scattering process. Münch (1948, 1950) investigated the broadening of spectral lines due to thermal motions and has found this effect in a Wolf-Rayet atmosphere. However, Compton shifts have been neglected. Chandrasekhar (1948) examined the shifts due to Compton scattering but neglected the Doppler shifts and used a Taylor series expansion (to the first term). We extended this work to the spherically symmetric geometry and by including the second derivative of the Taylor series (Peraiah 1990; Peraiah and Varghese 1991). Dirac studied Compton scattering for the first time and found that thermal motions produced a non-Doppler blueshift where frequencies would be larger than the red Compton shift. Therefore it would be interesting to study how Compton scattering changes the energy of a high frequency photon. Edmonds (1953) derived the spectral redistribution function to the second approximation. However, he solved the equation of transfer in plane parallel approximation using the first approximation of the redistribution function. He found that the non-Doppler blueshift due to the thermal motions is much larger than the Compton redshift for an optical depth of less than one which is appropriate in a Wolf-Rayet star. As this optical depth is much less than what is actually found in other objects, we would like to calculate the broadening due to Compton scattering in high optical depth cases and by adding the terms to include the second approximation (Edmonds 1954).

2. Solution of the equation of transfer with Compton broadening

The optical depth within the atmosphere is given by

$$d\tau = -N_e \sigma_e dZ \tag{1}$$

where dZ is length, N_e is electron density and σ_e is the Thompson scattering coefficient given by

$$\sigma_e = \frac{8\pi}{3}\frac{e^4}{m^2c^4} \tag{2}$$

where e is the electron charge, m its mass and c the velocity of light. The emission coefficient for Compton scattering by electrons in thermal motion is given by (see Edmonds 1953)

$$j(\nu,\tau,\mu) = N_e\sigma_e \int d\omega' . \frac{3}{4}(1+\cos^2\Theta) \int_0^\infty d\nu' I(\nu',\tau,\mu')\psi(\nu,\Theta,\nu'), \tag{3}$$

where primed quantities refer to the incident radiation, unprimed to the scattered radiation. And

$$\mu = \cos\theta. \tag{4}$$

Further, ν is the frequency of the radiation, $d\omega'$ is the increment of the solid angle about the direction of the incident radiation whose intensity is $I(\nu',\tau,\mu')$ and Θ the angle of scattering, is given by

$$\cos\Theta = \mu_1\mu_2 + \left[(1-\mu_1^2)(1-\mu_2^2)\right]^{1/2}\cos(\varphi-\varphi') \tag{5}$$

The spectral distribution function for scattered radiation is given, to the second approximation (see Edmonds 1953) as,

$$\psi(\nu,\Theta,\nu') = \frac{mc}{4\pi}\left[4\pi mkT(1-\cos\Theta)\right]^{-1/2}\frac{1}{\nu'}\left[1-\frac{3}{2}\left(\frac{\nu'-\nu}{\nu}\right)\right]\times$$
$$\exp\left\{\frac{-mc^2}{4kT(1-\cos\Theta)}\left[\frac{\nu'-\nu}{\nu}-\frac{h\nu'}{mc^2}(1-\cos\Theta)\right]^2\left[1+\frac{\nu'-\nu}{\nu}\right]^{-1}\right\}. \tag{6}$$

Here k is the Boltzmann's constant and h is the Planck's constant. For convenience we shall define

$$x = \frac{\nu-\nu_0}{\Delta} \tag{7}$$

$$x' = \frac{\nu'-\nu_0}{\Delta} \tag{8}$$

where Δ is the Doppler width.

The frequencies can be expressed in the form (see Edmonds 1953),

$$\alpha = \left[\frac{mc^2}{4kT}\right]^{1/2}\left(\frac{\nu-\nu_0}{\nu_0}\right)\left[1+\frac{\nu-\nu_0}{\nu_0}\right]^{1/2}$$
$$= -\left(\frac{mc^2}{4kT}\right)^{1/2}\left(\frac{\lambda'-\lambda_0}{\lambda_0}\right)\left[1-\frac{1}{2}\left(\frac{\lambda'-\lambda_0}{\lambda_0}\right)\right]^{1/2} \tag{9}$$

and

$$\alpha' = \left(\frac{mc^2}{4kT}\right)^{1/2}\left(\frac{\nu'-\nu_0}{\nu_0}\right)\left[1+\frac{\nu'-\nu_0}{\nu_0}\right]^{1/2}$$
$$= \left(\frac{mc^2}{4kT}\right)^{1/2}\left(\frac{\lambda'-\lambda_0}{\lambda_0}\right)\left[1+\frac{1}{2}\left(\frac{\lambda'-\lambda_0}{\lambda_0}\right)\right]^{1/2} \tag{10}$$

where λ and λ_0 are the wavelengths corresponding to ν and the fixed frequency ν_0 respectively.

Introducing x defined in equations (7) and (8), the quantities α and α' become,

$$\alpha = \frac{x}{\sqrt{2}}\left\{1+\sqrt{2}x\left(\frac{kT}{mc^2}\right)\right\}^{1/2} \tag{11}$$

and

$$\alpha' = \frac{x'}{\sqrt{2}}\left\{1+\sqrt{2}x'\left(\frac{kT}{mc^2}\right)^{1/2}\right\}^{1/2} \tag{12}$$

In terms of these variables, the emission coefficient $j(\alpha,\tau,\mu)$ is given by,

$$j(\alpha,\tau,\mu) = N_e\sigma_e \int \frac{d\omega'}{4\pi}\frac{\frac{3}{4}(1+\cos^2\Theta)}{[\pi(1-\cos\Theta)]^{1/2}}\int_{-\infty}^{+\infty} d\alpha' I(\alpha',\tau,\mu')$$
$$\left[1-\frac{3}{2}\left(\frac{4kT}{mc^2}\right)^{1/2}(\alpha'-\alpha)\right]\exp\left\{-\frac{(\alpha'-\alpha)^2}{(1-\cos\Theta)}+2\left(\frac{mc^2}{4kT}\right)^{1/2}\frac{h\nu_0}{mc^2}(\alpha'-\alpha)\right\} \tag{13}$$

3. The Equation of Transfer

Now the equation of transfer in plane parallel medium is given by

$$\mu\frac{\partial I(\alpha,\tau,\mu)}{\partial\tau} = I(\alpha,\tau,\mu) - \frac{j(\alpha,\tau,\mu)}{N_e\sigma_e} \tag{14}$$

We have to simplify the emission coefficient j so that a simple solution of the equation (14) can be found

We shall perform the integration over φ the azimuthal angle (see equation 5). The trigonometric functions involving the angle Θ are simplified and finally we obtain,

$$j(\alpha,\tau,\mu) = \frac{3}{16\pi}N_e\sigma_e\int\int d\mu' d\alpha' I(\alpha',\tau,\mu')Y_e\left[1-\frac{3}{2}\left(\frac{4kT}{mc^2}\right)^{1/2}(\alpha'-\alpha)\right]$$
$$\exp\left\{(\alpha'-\alpha)\left(\frac{mc^2}{kT}\right)^{1/2}\frac{h\nu_0}{mc^2}-(\alpha'-\alpha)^2\right\} \tag{15}$$

where

$$Y_e = 2+3M_1+\frac{27}{8}(2M_1^2+M_2^2)+\frac{91}{24}(2M_1^3+3M_1M_2^2)+$$
$$\frac{217}{48}(2M_1^4+6M_1M_2^2+\frac{3}{4}M_2^4) \tag{16}$$

where

$$M_1 = \mu_1\mu_2 \tag{17}$$

and

$$M_2 = \left\{(1-\mu_1^2)(1-\mu_2^2)\right\}^{1/2} \tag{18}$$

Equation (14) can now be written as

$$\mu\frac{dI(\alpha,\tau,\mu)}{d\tau} = \int_{-1}^{+1}\int_{-\infty}^{+\infty} d\mu_2 d\alpha I(\alpha',\tau,\mu')\Phi(\alpha,\mu,\alpha',\mu') - I(\tau,\mu,\alpha) \tag{19}$$

by defining

$$d\tau = -N_e\sigma_e dZ \tag{20}$$

$$\Phi(\alpha,\mu;\alpha',\mu') = \frac{3}{16\pi}Y_s\left[1-\frac{3}{2}\left(\frac{4kT}{mc^2}\right)^{1/2}(\alpha'-\alpha)\right]$$
$$\exp\left\{-(\alpha'-\alpha)^2-\frac{h\nu_0}{mc^2}(\alpha'-\alpha)\left(\frac{mc^2}{KT}\right)^{1/2}\right\}. \tag{21}$$

4. Solution of the equation of transfer

The equation (19) can be solved by the procedure given in Peraiah and Wehrse (1978) or Wehrse and Peraiah (1979). The discrete equivalent of equation (19) is

$$\mathbf{M}_m(\mathbf{I}^+_{i,n+1}-\mathbf{I}^+_{i,n})+\tau_{n+1/2}\mathbf{I}^+_{i,n+1/2} = \frac{1}{2}\tau_{n+1/2}\left[\Phi^{++}_{i,j',n+1/2}\mathbf{a}^{++}_{j',n+1/2}\mathbf{CI}^+_{j',n+1/2}\right.$$
$$\left.+\Phi^{+-}_{i,j',n+1/2}\mathbf{a}^{+-}_{j',n+1/2}\mathbf{CI}^-_{j',n+1/2}\right] \tag{22}$$

and

$$\mathbf{M}_m(\mathbf{I}^-_{i,n}-\mathbf{I}^-_{i,n+1})+\tau_{n+1/2}\mathbf{I}^-_{i,n+1/2} = \frac{1}{2}\tau_{n+1/2}\left[\Phi^{-+}_{i,j',n+1/2}\mathbf{a}^{-+}_{j',n+1/2}\mathbf{CI}^+_{j',n+1/2}\right.$$
$$\left.+\Phi^{--}_{i,j',n+1/2}\mathbf{a}^{--}_{j',n+1/2}\mathbf{CI}^-_{j',n+1/2}\right] \tag{23}$$

where

$$\Phi^{++}_{i,j',n+1/2} = \Phi(\alpha_i,+\mu_1,\alpha_{j'},\mu_2) \tag{24}$$

and

$$\Phi^{+-}_{i,j',n+1/2} = \Phi(\alpha_i,+\mu_1;\alpha_{j'},\mu_2). \tag{25}$$

Similarly Φ^{-+},Φ^{--} are defined. Further more,

$$\mathbf{M}_m = \mu_{jk}\delta_{jk} \tag{26}$$

and

$$\mathbf{c} = c_{jk}\delta_{jk} \tag{27}$$

μ and c being the root and weight of the angle quadrature.

Equations (22) and (23) can be combined for all the frequency points in the line and discrete equations can be written as,

$$\mathbf{M}\left[\mathbf{I}^+_{n+1}-\mathbf{I}^+_n\right]+\tau_{n+1/2}\mathbf{I}^+_{n+1/2} = \frac{1}{2}\tau_{n+1/2}\left[\Phi^{++}\mathbf{W}^{++}\mathbf{I}^+ + \Phi^{+-}\mathbf{W}^{+-}\mathbf{I}^-\right]_{n+1/2} \tag{28}$$

and

$$\mathbf{M}\left[\mathbf{I}^-_n-\mathbf{I}^-_{n+1}\right]+\tau_{n+1/2}\mathbf{I}^-_{n+1/2} = \frac{1}{2}\tau_{n+1/2}\left[\Phi^{-+}\mathbf{W}^{-+}\mathbf{I}^+ + \Phi^{--}\mathbf{W}^{--}\mathbf{I}^-\right]_{n+1/2} \tag{29}$$

where

$$\mathbf{I}^+_{n+1/2} = \left[I_1 I_2 I_3 \ .. \ I_l\right]^T_{n+1/2} \tag{30}$$

and

$$W_k = a_i c_j, a_i = \frac{A_i\Phi_i}{\sum_{i'=-I}^{I}A_i\Phi_{i'}} \tag{31}$$

$$k = j+(i-1)m \quad 1\le k\le K = mI \tag{32}$$

where

m = total number of angle points, i = running index of frequency points, j = running index of the angle points, I = total number of frequency points.

$$\mathbf{M} = \begin{pmatrix} \mathbf{M}_m & & & \\ & \mathbf{M}_m & & \\ & & \ddots & \\ & & & \mathbf{M}_m \end{pmatrix} \tag{33}$$

and

$$\mathbf{c} = \begin{pmatrix} \mathbf{c} & & \\ & \mathbf{c} & \\ & & \ddots \end{pmatrix}. \tag{33a}$$

The r and t operators are given by

$$\mathbf{t}(n+1,n) = \mathbf{G}^{+-}\left[\Delta^{+}\mathbf{A} + \mathbf{g}^{+-}\mathbf{g}^{-+}\right] \tag{34}$$

$$\mathbf{t}(n,n+1) = \mathbf{G}^{-+}\left[\mathbf{A}^{-}\mathbf{D} + \mathbf{g}^{-+}\mathbf{g}^{+-}\right] \tag{35}$$

$$\mathbf{r}(n+1,n) = \mathbf{G}^{-+}\mathbf{g}^{-+}\left[\mathbf{I} + \Delta^{+}\mathbf{A}\right] \tag{36}$$

$$\mathbf{r}(n,n+1) = \mathbf{G}^{+-}\mathbf{g}^{+-}\left[\mathbf{I} + \Delta^{-}\mathbf{D}\right] \tag{37}$$

wher I is the unit matrix and cell operators are

$$\Sigma^{+}_{n+1/2} = \mathbf{G}^{+-}\left[\Delta^{+}\mathbf{S}^{+}_{n+1/2} + \mathbf{g}^{+-}\Delta^{-}\mathbf{S}^{-}_{n+1/2}\right]\tau_{n+1/2} \tag{38}$$

$$\Sigma^{-}_{n+1/2} = \mathbf{G}^{-+}\left[\Delta^{-}\mathbf{S}^{-}_{n+1/2} + \mathbf{g}^{-+}\Delta^{+}\mathbf{S}^{+}_{n+1/2}\right]\tau_{n+1/2} \tag{39}$$

where

$$\mathbf{G}^{+-} = \left[\mathbf{I} - \mathbf{g}^{+-}\mathbf{g}^{-+}\right]^{-1} \tag{40}$$

$$\mathbf{G}^{-+} = \left[\mathbf{I} - \mathbf{g}^{-+}\mathbf{g}^{+-}\right]^{-1} \tag{41}$$

$$\mathbf{g}^{+-} = \frac{1}{2}\tau_{n+1/2}\Delta^{+}\mathbf{Y}_{-} \tag{42}$$

$$\mathbf{g}^{-+} = \frac{1}{2}\tau_{n+1/2}\Delta^{-}\mathbf{Y}_{+} \tag{43}$$

$$\mathbf{D} = \mathbf{M} - \frac{1}{2}\tau_{n+1/2}\mathbf{Z}_{-} \tag{44}$$

$$\mathbf{A} = \mathbf{M} - \frac{1}{2}\tau_{n+1/2}\mathbf{Z}_{+} \tag{45}$$

$$\Delta^{+} = \left[\mathbf{M} + \frac{1}{2}\tau_{n+1/2}\mathbf{Z}_{+}\right]^{-1} \tag{46}$$

$$\Delta^{-} = \left[\mathbf{M} + \frac{1}{2}\tau_{n+1/2}\mathbf{Z}_{-}\right]^{-1} \tag{47}$$

$$\mathbf{Z}_{+} = -\frac{1}{2}\left(\Phi^{++}\mathbf{W}^{++}\right)_{n+1/2} \tag{48}$$

$$\mathbf{Z}_{-} = -\frac{1}{2}\left(\Phi^{--}\mathbf{W}^{--}\right)_{n+1/2} \tag{49}$$

$$\mathbf{Y}_{+} = \frac{1}{2}\left(\Phi^{-+}\mathbf{W}^{-+}\right)_{n+1/2} \tag{50}$$

$$\mathbf{Y}_{-} = \frac{1}{2}\left(\Phi^{+-}\mathbf{W}^{+-}\right)_{n+1/2}. \tag{51}$$

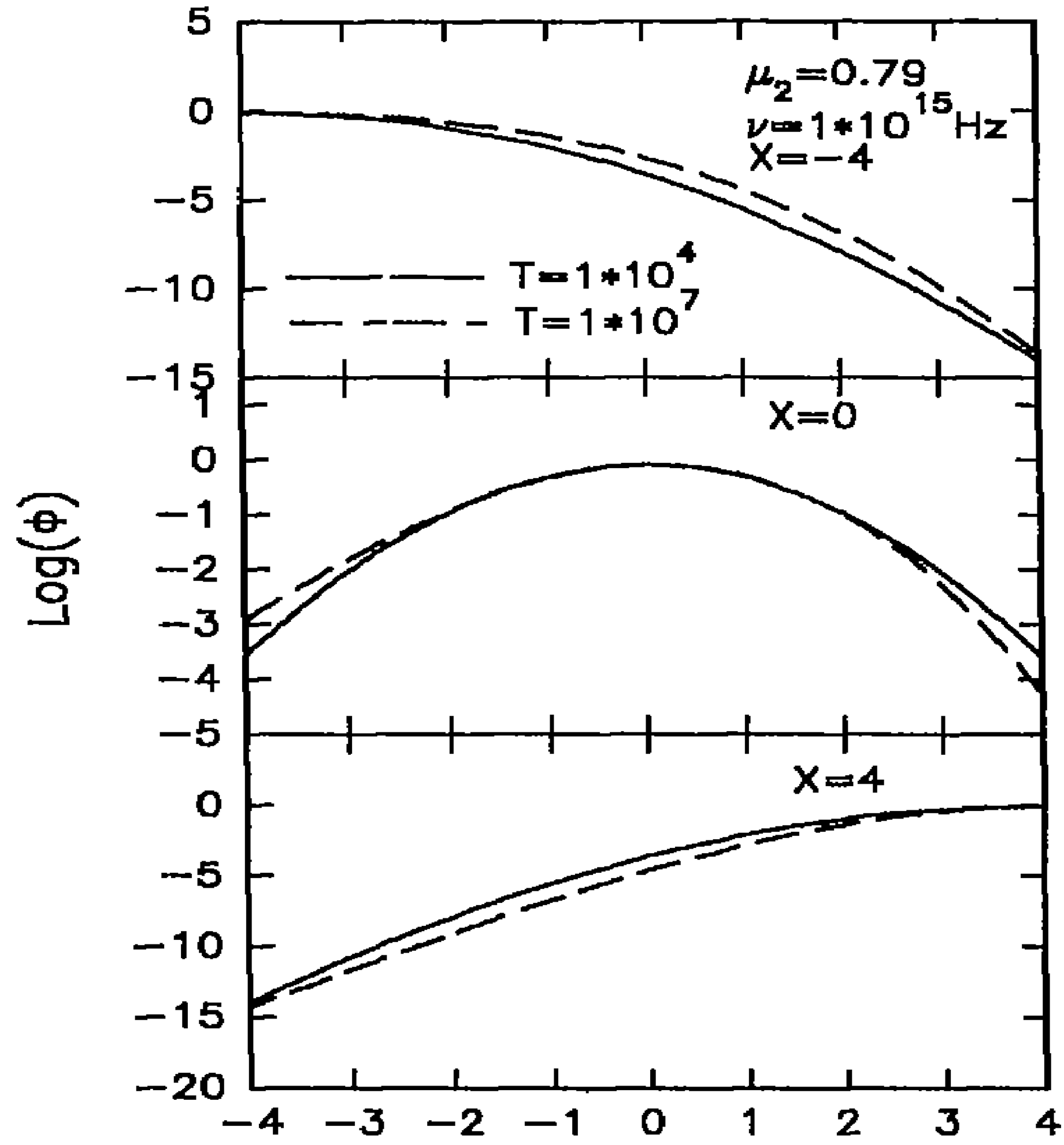

Fig 1. The scattering function Φ is plotted.

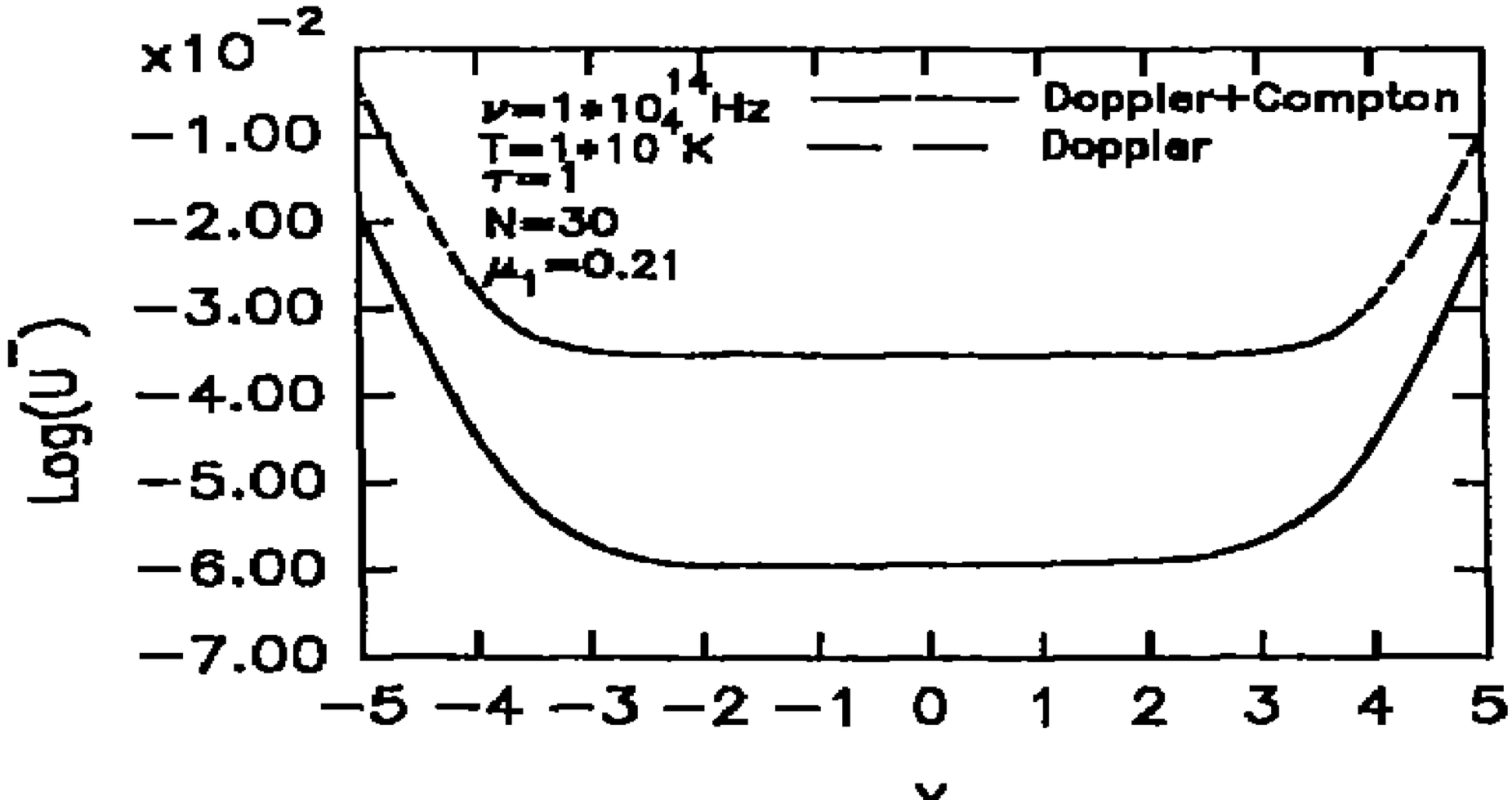

Fig 2. The intensity profile of U^- is given at $\tau = \tau_{max} = 1$.

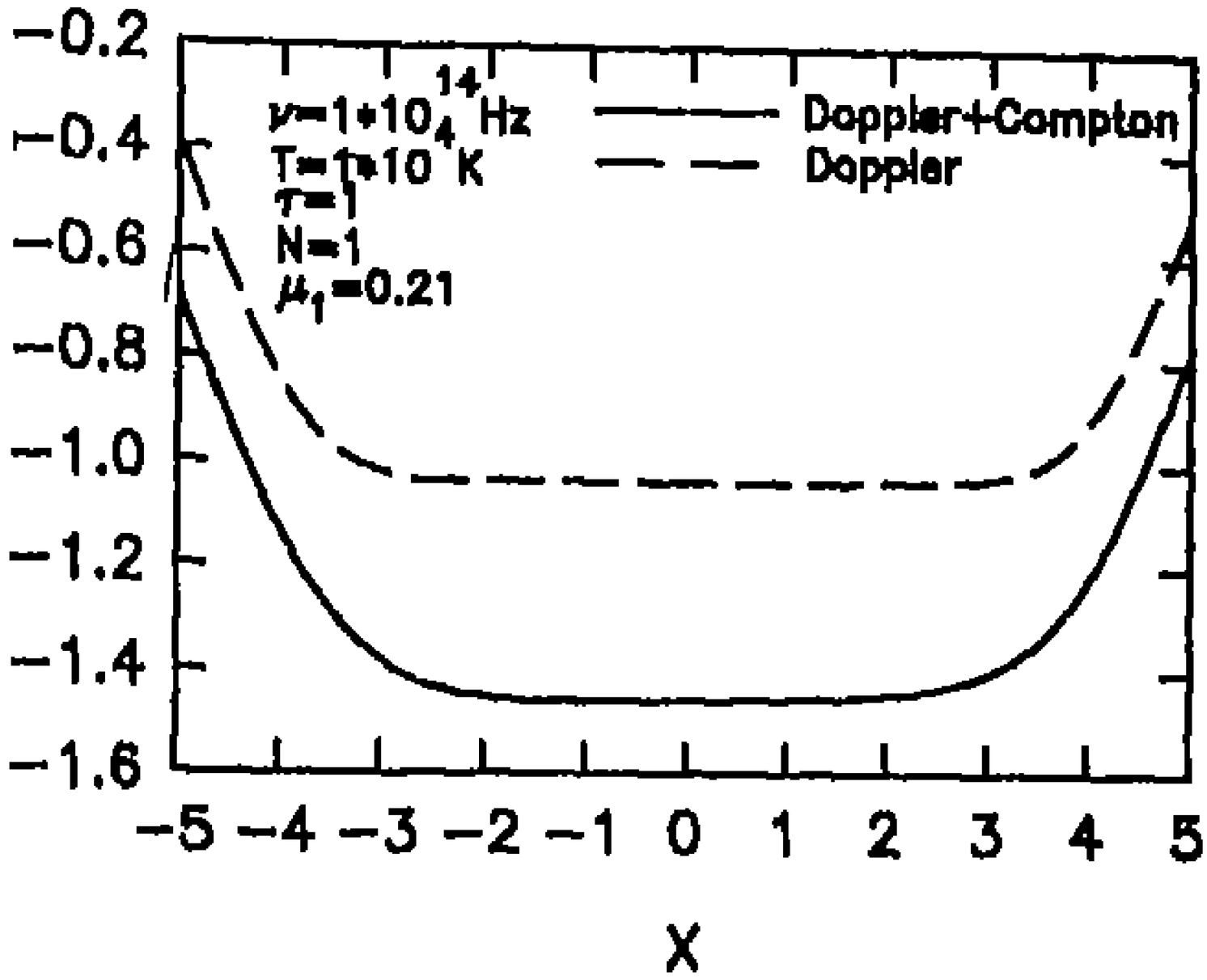

Fig 3. Same as those given in Fig. 2 at $\tau = 0$ with $\tau_{max} = 1$.

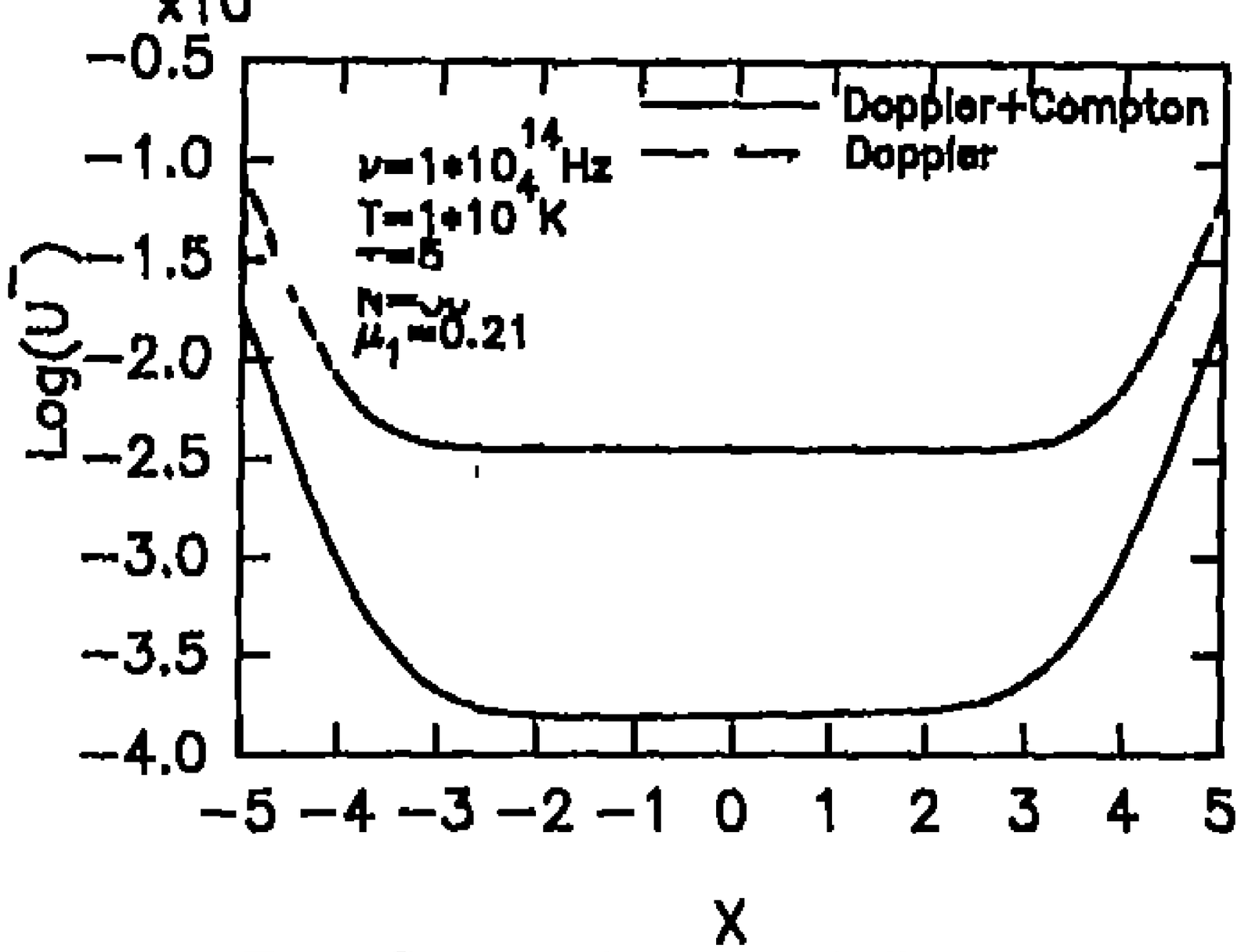

Fig 4. Same as those given in Fig. 2 at $\tau = \tau_{max} = 5$

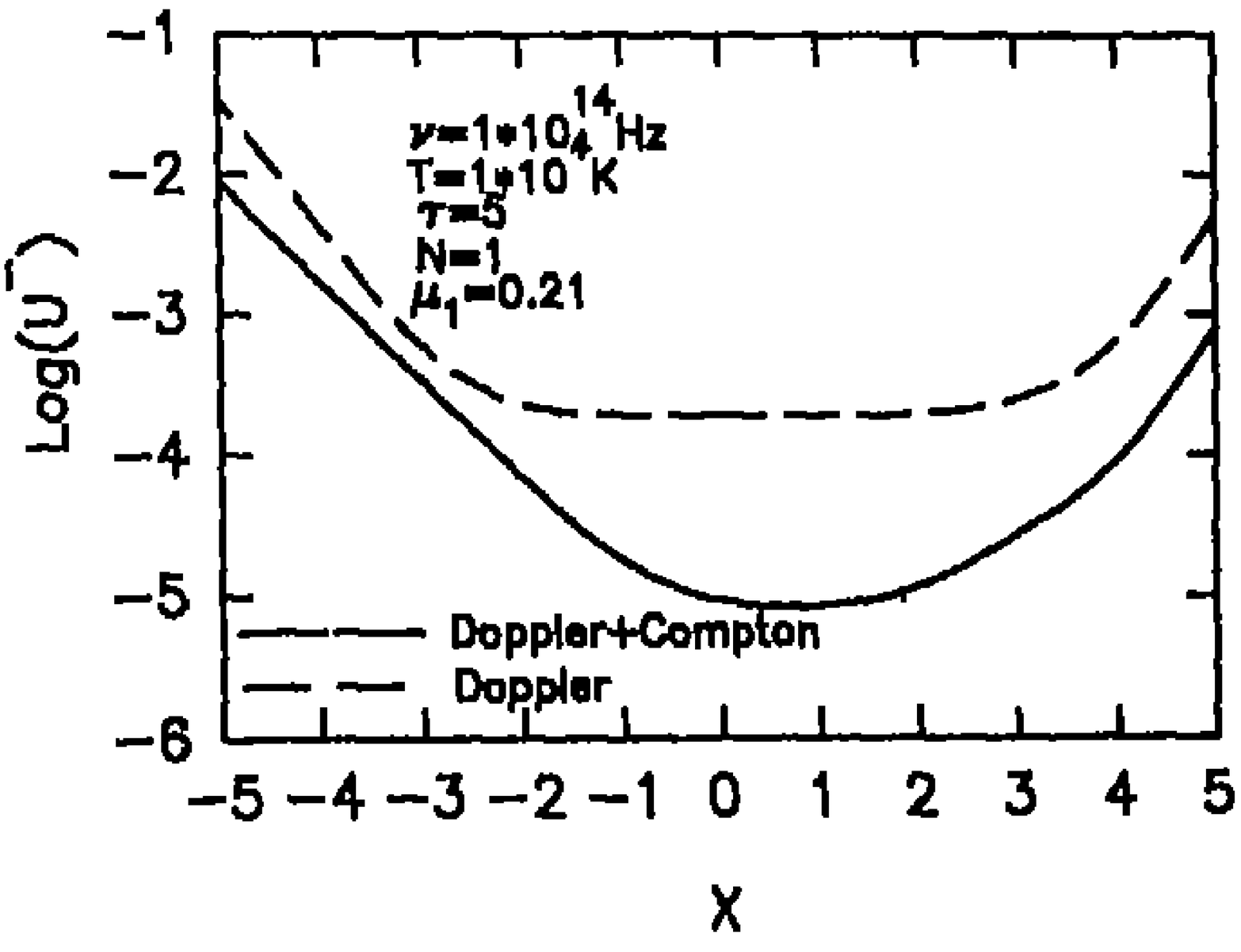

Fig 5. Same as those given in Fig. 4 at $\tau = 0$ with $\tau_{max} = 5$.

5. Results and Discussions

It is interesting to find out how the scattering function Φ behaves. We have chosen the normalized frequency points X = -4 to +4 (+1) with corresponding trapezoidal weights. We have chosen two angle points on the Gauss-Legendre quadrature (0,1). In Fig.1, we plotted log Φ for X = -4, X = 0 and X = +4. It is easily seen that the probability that a photon emitted at X = -4 are reappearing at X = 0 is considerably higher than that emitted at X = +4 and reappearing at X = 0. However in the case of the photons emitted either at X = -4 or +4 their probability of reappearing at X = +4 and -4 respectively is extremely small. The photons emitted at X = 0 would appear at X = $\pm$4 more strongly although at X = -4, the probability is slightly higher than at X = +4.

In Fig.2, we have plotted the U^- at $\tau = \tau_{max}$ for $\tau = 1$. We see that the dotted (Doppler) curve and continuous curve (Doppler + Compton) differ considerably. In Fig.3, we have shown U^- at $\tau = 0$. The intensities are reduced but show the same tendency of variation as those in Fig.2.

In Fig.4, we have shown the profiles of U^- at $\tau = \tau_{max}$ for $\tau = 5$ and we notice slight asymmetry together with increase in the broadening. The asymmetry and broadening are increased further in the results shown in Fig.5, for $\tau = 0$. Therefore for $\tau > 1$, Compton scattering introduces more broadening and increases asymmetry.

References

Munch,G., 1948, Astrophys.J., 108, 116.

Munch,G., 1950,Astrophys.J., 112, 66.

Edmonds, Jr. F.N., 1953,Astrophys.J., 117, 298.

Edmonds, Jr.F.N.,1954, Astrophys.J., 119, 58.

Chandrasekhar, S., 1948,Proc.R.Soc.London.A., 191, 508.

Peraiah,A., 1990,J.Astron.& Astrophys., 11,193.

Peraiah,A., Varghese,B.A.,1991,Publ.Astr.Soc.Japan,42,No.5.